Artificial viscosity Discontinuous Galerkin Spectral Element Method for the Baer-Nunziato equations

C. Redondo, F. Fraysse, G. Rubio and E. Valero

Abstract This paper is devoted to the numerical discretization of the hyperbolic two-phase flow model of Baer and Nunziato. Special attention is paid to the discretization of interface flux functions in the framework of Discontinuous Galerkin approach, where care has to be taken to efficiently approximate the non-conservative products inherent to the model equations. A discretization scheme is proposed in a Discontinuous Galerkin framework following the criterion of Abgrall. A stabilization technique based on artificial viscosity is applied to the high-order Discontinuous Galerkin method and tested on a bench of discontinuous test cases.

1 Introduction

In this work a high order discretization method for the hyperbolic two-phase flow model of Baer and Nunziato [3] is introduced. The model is composed of seven equations in one-dimension: continuity, momentum and energy balance for each phase and a convection equation for the volume fraction. It does not make any assumption on mechanical, thermal or chemical equilibrium, thus, two pressures, velocities and temperatures are present. The main challenge of this set of equations is that it cannot be cast in conservative (or divergence) form because of the presence of non-conservative products. As a consequence, classical Rankine-Hugoniot conditions cannot be used to define the jumps across the contact discontinuities and shocks. This issue has remained challenging for a long time but recently some authors published different methods in order to treat these additional terms [29, 24, 30, 32].

C. Redondo, G. Rubio and E. Valero
School of Aeronautics (ETSIAE Universidad Politécnica de Madrid). Spain. e-mail: carlos.redondo@upm.es, e-mail: g.rubio@upm.es, e-mail: eusebio.valero@upm.es

F. Fraysse
RS2N. France. e-mail: francois.fraysse@rs2n.eu

On the one hand, most works in the literature use a finite volume (FV) methodology, often limited to second-order of accuracy, to discretize the Baer-Nunziato equations, see [11] for a review. Attempts to reconstruct Finite Volume methodology to higher order usually suffer from a lack of compactness, which is a bottleneck for massive parallel implementation. On the other hand, discontinuous Galerkin (DG) methods take the advantages of FV approach (conservation, interface jumps, compactness) but naturally allow the solution to be represented by a high-order polynomial. DG methods, firstly introduced in [27], have emerged in recent years as an efficient and flexible method to solve convection dominated problems [8]. A nodal variant of the DG technique that uses a quad/hexa mesh topology and tensor product expansions for the polynomial spaces is known as Discontinuous Galerkin Spectral Element Method (DGSEM), as detailed in Kopriva [22]. The DGSEM has been successfully used in a wide range of applications, in particular to model one phase compressible flows [5, 26, 20, 21]. Recently some DGSEM formulations able to solve the Baer-Nunziato equations in the presence of discontinuities have been introduced by the authors [11]. One of the important aspects of this development is the special treatment to avoid oscillations in the vicinity of shocks and contact discontinuities. The method builds on work by Persson *et al.* [25] and uses a simple artificial viscosity technique [34, 4, 17, 16] to stabilize the solution. In this work the most successful of the formulations proposed in [11] is introduced and analyzed in detail in a one-dimensional framework.

The paper is organized as follows: in Sec. 2 the discretization of the Baer-Nunziato equations is presented. The DG method is detailed as well as the upwind fluxes, the treatment of the non-conservative products and the stabilization method. In Sec. 3, the developed numerical scheme is tested using a bench of one-dimensional test cases.

2 Discretization of the two-phase two-pressure model of Baer and Nunziato

The one-dimensional set of Baer-Nunziato equations reads:

$$\frac{\partial \mathbf{U}}{\partial t} + \frac{\partial \mathbf{F}(\mathbf{U})}{\partial x} + \mathbf{H}(\mathbf{U}) \frac{\partial \alpha_l}{\partial x} = 0, \tag{1}$$

where

$$\mathbf{U} = \begin{bmatrix} \alpha_l \\ \alpha_l \rho_l \\ \alpha_l \rho_l u_l \\ \alpha_l \rho_l E_l \\ \alpha_g \rho_g \\ \alpha_g \rho_g u_g \\ \alpha_g \rho_g E_g \end{bmatrix} \quad \mathbf{F}(\mathbf{U}) = \begin{bmatrix} 0 \\ \alpha_l \rho_l u_l \\ \alpha_l \rho_l u_l^2 + p_l \\ \alpha_l \rho_l u_l H_l \\ \alpha_g \rho_g u_g \\ \alpha_g \rho_g u_g^2 + p_g \\ \alpha_g \rho_g u_g H_g \end{bmatrix} \quad \mathbf{H}(\mathbf{U}) = \begin{bmatrix} u_{int} \\ 0 \\ -p_{int} \\ -p_{int} u_{int} \\ 0 \\ p_{int} \\ p_{int} u_{int} \end{bmatrix}$$

This system of equations is closed with an equation of state for each phase $m = g,l$ (gas and liquid) relating the internal energy $e_m = E_m - 0.5u_m^2$ to the density ρ_m and pressure p_m, the saturation condition $\alpha_l + \alpha_g = 1$ (liquid and gas volume fractions) and finally appropriate interfacial pressure and velocity. In this work, stiffened gas equation is considered for the liquid phase, $p_m = \rho_m e_m(\gamma_m - 1) + \pi_m$, and perfect gas law for the gas phase ($\pi_g = 0$). The interfacial quantities are set according to the choice of Baer and Nunziato: $u_{int} = u_l, p_{int} = p_g$.

2.1 Discontinuous Galerkin Spectral Element Method

Discontinuous Galerkin methods and, in particular the nodal variant DGSEM, were originally developed to solve conservation laws. Unfortunately, it is not possible to cast the Baer-Nunziato equations in conservative form due to the presence of non-conservative products of the form $\mathbf{H}(\mathbf{U})\frac{\partial \alpha_l}{\partial x}$. The difficulty of integrating this term over a control volume arises in the presence of a discontinuity in the volume fraction. As a result, some modifications from the original DGSEM are required. It should be noticed that the scope of this work is limited to one-dimensional approximations.

Let us rewrite the Baer-Nunziato equations,

$$\mathbf{U}_t + \mathbf{F}_x + \mathbf{H}(\alpha_l)_x = 0, \quad x \in \Omega, \tag{2}$$

where $\mathbf{U}$ is the solution and $\mathbf{U}_t$ denotes its temporal derivative. The flux function is $\mathbf{F}$, while $\mathbf{F}_x$ denotes its spatial derivative and the non conservative flux is denoted by $\mathbf{H}(\alpha_l)_x$ (notice that $\alpha_l = \mathbf{U}(1)$). In the following and to simplify the notation α_l will be shortened to α.

Discontinuous Galerkin methods tessellate the physical domain Ω into non overlapping subdomains Ω_k. The residual is forced to be orthogonal to the approximation space locally within each element,

$$\int_{\Omega_k} (\mathbf{U}_t + \mathbf{F}_x + \mathbf{H}\alpha_x)\, \psi dx = 0, \tag{3}$$

where ψ is an arbitrary locally smooth function. The physical domain Ω_k, of size Δx_k, is mapped into the computational domain, which in 1D is $[-1,1]$,

$$\frac{\Delta x_k}{2} \int_{-1}^{1} \mathbf{U}_t \psi d\xi + \int_{-1}^{1} \mathbf{F}_\xi \psi d\xi + \int_{-1}^{1} \mathbf{H}\alpha_\xi \psi d\xi = 0. \tag{4}$$

The solution and the fluxes are approximated by polynomials of degree N. A characteristic of the DGSEM is that it approximates both the solution and the fluxes with the same polynomial degree, e.g.,

$$\mathbf{U}(\xi,t) \approx \mathbf{U}^N(\xi,t) = \sum_{i=0}^{N} \mathbf{U}^N(\xi_i,t)\ell_i(\xi). \tag{5}$$

This approximation results in a computationally efficient method with higher aliasing error. The approximation is nodal, therefore ℓ_i are Lagrange polynomials while ξ_i are chosen to be Legendre-Gauss nodes. As a result, $\mathbf{U}^N(\xi_i,t)$ is the solution at the Legendre-Gauss nodes. The nodal values of the fluxes $\mathbf{F}^N(\xi_i,t)$ and $\mathbf{H}^N(\xi_i,t)$ are computed evaluating the solution at the nodes. As the method is Galerkin, the test function can also be written as a polynomial $\psi = \sum_{i=0}^{N} \psi_i \ell_i(\xi)$. Now, substituting the polynomial expressions in Eq. 4 and taking into account that the coefficients ψ_i are linearly independent we get,

$$\begin{aligned} &\frac{\Delta x_k}{2}\int_{-1}^{1} \mathbf{U}_t^N \ell_j(\xi) d\xi + \int_{-1}^{1} \mathbf{F}_\xi^N \ell_j(\xi) d\xi \\ &+ \int_{-1}^{1} \mathbf{H}^N \alpha_\xi^N \ell_j(\xi) d\xi \ = 0, \quad j = 0,1,\ldots,N. \end{aligned} \tag{6}$$

Equation 6 is integrated by parts to separate volume from surface contributions,

$$\begin{aligned} &\frac{\Delta x_k}{2}\int_{-1}^{1} \mathbf{U}_t^N \ell_j(\xi) d\xi + \left(\mathbf{F}^N + \mathbf{H}^N \alpha^N\right) \ell(\xi)\big|_{-1}^{1} - \int_{-1}^{1} \mathbf{F}^N \ell_j'(\xi) d\xi \\ &- \int_{-1}^{1} \mathbf{H}_\xi^N \alpha^N \ell_j(\xi) d\xi - \int_{-1}^{1} \mathbf{H}^N \alpha^N \ell_j'(\xi) d\xi = 0, \quad j = 0,1,\ldots,N. \end{aligned} \tag{7}$$

It should be noticed that the computation of the volume fraction derivative, α_ξ, inside the control volume is not required after the integration by parts. In order to obtain a completely discrete equation, the integrals are approximated using Gaussian quadrature. In the DSGEM the interpolation nodes are used as quadrature nodes,

$$\begin{aligned} &\frac{\Delta x_k}{2}\dot{\mathbf{U}}_j^N w_j + \left(\mathbf{F}^N + \mathbf{H}^N \alpha^N\right) \ell_j(\xi)\big|_{-1}^{1} - \sum_{i=0}^{N} \mathbf{F}_i^N \ell_j'(\xi_i) w_i \\ &- \sum_{i=0}^{N} \mathbf{H}_i^N \alpha_j^N \ell_i'(\xi_j) w_j - \sum_{i=0}^{N} \mathbf{H}_i^N \alpha_i^N \ell_j'(\xi_i) w_i = 0, \quad j = 0,1,\ldots,N. \end{aligned} \tag{8}$$

Finally, the elements are coupled through the definition of a numerical interface flux,

$$\begin{aligned} &\frac{\Delta x_k}{2}\dot{\mathbf{U}}_j^N w_j + \left(\mathbf{F}^{N*} + \mathbf{H}^N \alpha^{N*}\right) \ell_j(\xi)\big|_{-1}^{1} - \sum_{i=0}^{N} \mathbf{F}_i^N \ell_j'(\xi_i) w_i \\ &- \sum_{i=0}^{N} \mathbf{H}_i^N \alpha_j^N \ell_i'(\xi_j) w_j - \sum_{i=0}^{N} \mathbf{H}_i^N \alpha_i^N \ell_j'(\xi_i) w_i = 0, \quad j = 0,1,\ldots,N. \end{aligned} \tag{9}$$

The numerical flux $\mathbf{F}^{N*}$ and α^{N*} is a function of the element and its immediate neighbor (or a physical boundary). To calculate its value, a Riemann problem should be solved [33]. The Riemann solver calculates a value for the fluxes, taking into account the values at each side of the discontinuity and the directions of transfer of information in the equation. More information about the numerical flux computation

will be given in the next section. Having obtained a suitable discrete expression for each elemental contribution, it suffices to sum over all elements in the mesh and apply the boundary conditions weakly to finalize the DGSEM method, see details in Kopriva [22].

2.2 Interface flux approximation. Criterion of Abgrall

In this section we present the approximate Riemann solver employed to compute the intercell fluxes $\mathbf{F}^{N*}$ and α^{N*} of the 7-equation Baer-Nunziato two-phase flow model.

For the conservative flux $\mathbf{F}^{N*}$, the Rusanov flux is chosen. The Rusanov flux [23, 28] only uses one wave speed S_{max} which is the maximum absolute eigenvalue of left and right states of the Jacobian matrix. The main advantage of the Rusanov flux is its simplicity and low dependence on the eigenstructure of the flux Jacobian. Thus, it is particularly easy to implement when the flux Jacobian is difficult to formulate, for example when a complex equation of state is used. Its main disadvantage is its high diffusion of discontinuities, in particular the contact discontinuities. This effect is diminished if a high order approximation is used.

The volume fraction interface flux approximation α^{N*} will be computed following the so-called Abgrall criterion. The criterion of Abgrall [1] states that a two-phase flow uniform in velocity and pressure should remain uniform in these variables with time evolution. In order to satisfy the criterion of Abgrall for the Rusanov flux, some choices are to be made for the flux $\mathbf{F}^{N*}$ and the liquid volume fraction at the interface α^{N*}. The classical flux holds the conservative part of the system and is here augmented to hold a contribution from the liquid volume fraction equation, denoted by $F^*_{1_b}$. The scheme is chosen such that:

$$\begin{cases} F^*_{1_b} = -\dfrac{S_{max}}{2}(\alpha_R - \alpha_L) \\ \alpha^{N*} = \dfrac{\alpha_R + \alpha_L}{2} \end{cases} \quad \text{Rusanov flux with Abgrall criterion} \tag{10}$$

It should be noticed that an interpolation from the interior Gauss points to the interface points ± 1 is required to obtain left and right states (e.g. α_L,α_R) for the intercell flux computation.

2.3 Stabilization using an artificial viscosity method

The upwind scheme presented earlier may yield high oscillations in the vicinity of discontinuities due to Gibbs phenomena [14]. The objective here is to search for a method that detects the occurrence of the Gibbs phenomena and attenuates it. Several methods can be found in the literature to stabilize the solution in the presence

of discontinuities. Classical limiters work well in order to avoid the local creation of extrema, however they severely degrade the accuracy, often reduced to one in the entire cell. Artificial viscosity methods, firstly introduced in the scope of finite differences in the fifties by von Neumann and Richtmyer [34], add a controlled amount of viscosity to the governing equations in the vicinity of strong gradients, such as shock waves or contact discontinuities. In this way the discontinuity may be resolved in the space of interpolating polynomials. Other variants of artificial viscosity methods exist as well. A particularly important one is the method of Spectrally Vanishing Viscosity (SVV) [31, 18], which is similar in spirit, but the smoothing is limited to the high frequency components of the solution.

In this work, we construct an stabilization method for the multiphase flow based on the single phase work of Persson *et al.* [25], where the mitigation is attained through an artificial viscosity technique. The new set of equations, with the artificial viscosity term included, reads:

$$\frac{\partial \mathbf{U}}{\partial t} + \frac{\partial \mathbf{F}}{\partial x} + \mathbf{H}\frac{\partial \alpha_l}{\partial x} = \frac{\partial}{\partial x}\left(\varepsilon \frac{\partial \mathbf{U}}{\partial x}\right) \tag{11}$$

Then the discontinuity should spread over a layer of thickness ε. The definition of the parameter ε, that controls the amount of viscosity introduced, as well as the definition of a sensor to capture the regions where the stabilizing viscosity should be added, are key aspects in the development of the artificial viscosity method.

The discontinuity sensor is built following [25]. Spectral methods represent the solution of the problem as a sum of basis functions multiplied by some coefficients. In particular the DGSEM uses the Legendre orthogonal polynomials as a basis and therefore a one dimensional solution of order N, can be represented in each element as a sum of local modes,

$$\mathbf{U}^N(x) = \sum_{i=0}^{N} \tilde{\mathbf{U}}_i^N L_i(x), \tag{12}$$

where $\tilde{\mathbf{U}}_i^N$ is the projection of the solution onto the Legendre orthogonal polynomial $L_i(x)$. It should be noticed that the DGSEM is a nodal method, and therefore the coefficients, $\mathbf{U}_i^N$, obtained in Eq. 9 are the values of the solution at the collocation nodes and not the modal coefficients $\tilde{\mathbf{U}}_i^N$. However, they can be computed from the nodal values as:

$$\mathscr{V}\tilde{\mathbf{U}}^N = \mathbf{U}^N, \tag{13}$$

where matrix $\mathscr{V}$ is a generalized Vandermonde matrix [15]. A particularity of spectral methods is that for smooth solutions the coefficients $\tilde{\mathbf{U}}_i$ decay very quickly (exponential convergence), while the convergence rate is poor (algebraic convergence) for non smooth solutions [13, 6].

A truncated expansion of order $N-1$ of the solution, $\mathbf{U}^N(x)$, is also constructed as:

$$\hat{\mathbf{U}}^{N-1}(x) = \sum_{i=0}^{N-1} \tilde{\mathbf{U}}_i^N L_i(x). \tag{14}$$

The difference between the truncated expansion of the solution, $\hat{\mathbf{U}}^{N-1}$, and the solution itself, $\mathbf{U}^N$, is small for smooth solutions and big for discontinuous solutions due to spectral convergence. In order to measure the difference between the two functions the following indicator is computed within each element:

$$s = \log_{10} \max \left(\frac{(\mathbf{U}^N - \hat{\mathbf{U}}^{N-1}, \mathbf{U}^N - \hat{\mathbf{U}}^{N-1})}{(\mathbf{U}^N, \mathbf{U}^N)} \right), \tag{15}$$

where $(u,v) = \int_{-1}^{1} uvdx$ represents the usual L^2 inner product and can be approximated using Legendre-Gauss quadrature. It should be noticed that the maximum value among all the equations is taken, which is justified as the objective of the indicator is to capture discontinuities in any of the equations.

Finally, ε, the amount of viscosity imposed in each element, is computed as:

$$\varepsilon = \begin{cases} 0 & \text{if } s < s_0 - \kappa \\ \dfrac{\varepsilon_0}{2} \left(1 + \sin \dfrac{\pi(s - s_0)}{2\kappa} \right) & \text{if } s_0 - \kappa \leq s \leq s_0 + \kappa \\ \varepsilon_0 & \text{if } s > s_0 + \kappa \end{cases} \tag{16}$$

In this work, the values of $\varepsilon_0 = \frac{h}{(N+1)}$ (being h the size of the elements), $s_0 = \log_{10} \frac{1}{(N+1)^4}$ and $\kappa = 5$ were chosen empirically and demonstrated very satisfactory results. As it is explained in [25], the selection of these values for the parameters introduces viscosity only when the solution is not continuous and the profiles of the discontinuities are sharp but smooth. The effectiveness of these parameters to correctly capture the discontinuities and stabilize the solution in the multiphase framework will be shown in Sec. 3.

The artificial viscosity method produces an *a posteriori* stabilization, i.e. the solution is not stabilized until the oscillation is generated. In general there is no problem with this, however if the amplitude of the oscillation is too high it can transiently produce unphysical values of the variables, e.g. negative densities or volume fractions outside the interval $[0,1]$. This is inadmissible as the computation of some quantities, e.g. the speed of sound, would result in invalid operations. The development of a robust artificial viscosity method requires the introduction of relaxation iterations. If any of the aforementioned variables acquire an unphysical value as a result of an oscillation, a relaxation iteration is performed instead of the regular iteration. In a regular iteration, the time derivative of the solution is computed with Eq. 11, while in a relaxation iteration only the diffusive terms,

$$\frac{\partial \mathbf{U}}{\partial t} = \frac{\partial}{\partial x} \left(\varepsilon \frac{\partial \mathbf{U}}{\partial x} \right), \tag{17}$$

are computed. It should be noticed that relaxation iterations do not produce an advance in physical time but only a filtering of the solution.

A comment should be made about the major drawback of the artificial viscosity approach: the reduction in the stable time step for explicit time stepping schemes [19, 7]. The scaling of the explicit time step is given by:

$$\Delta t \sim \left(S_{max}N^2/h + ||\varepsilon||_{L^\infty}N^4/h^2\right)^{-1}, \tag{18}$$

where S_{max} is the absolute value of the largest characteristic velocity, ε is the magnitude of the viscosity, h is the size of the element and N is the approximation's polynomial degree [15]. Therefore if the maximum value of the artificial viscosity is used (see Eq. 16), the time step is given by:

$$\Delta t \sim \left(N^2/h(S_{max}+N)\right)^{-1}, \tag{19}$$

therefore S_{max} is increased by N because of the artificial viscosity method. To overcome this limitation, several approaches are available. The cost of explicit time stepping methods can be reduced, for example, by using local time stepping [36] or adaptive time stepping [9] techniques. A different approach is to circumvent the time stability limit by using implicit methods [35]. Finally, a similar effect to artificial viscosity can be obtained by filtering the solution, thus not affecting the time stability limit [12, 15].

The derivation of the DGSEM performed in Sec. 2.1 does not include second order derivatives. However, the stabilization using artificial viscosity requires them. Several methods are available in the literature to perform the discretization of elliptic problems, see [2] for a thorough review. In this work the Symmetric Interior Penalty Discontinuous Galerkin [10] has been chosen to discretize the second order derivatives.

3 Numerical experiments

In this section, our aim is to test the developed method. Several shock tube problems are used to test the capturing properties of the scheme in the presence of discontinuities. We consider seven test problems which are classical benchmark, see for instance [32]. The initial data consists of two constant states separated by a discontinuity located at $x = x_0$, all the parameters are listed in Table 1. Transmissive boundary conditions are imposed at $x = 0$ and $x = 1$.

In test 1 the liquid phase wave pattern consists of a left rarefaction, a right shock wave and a right traveling liquid contact, while the gas phase consists of a left rarefaction, a contact and a right shock wave. The equations of state for both phases are assumed ideal, with $\gamma_g = \gamma_l = 1.4$. Test 2 is more demanding than test 1 as it includes

(a) EOS parameters and initial discontinuity position

	Test 1	Test 2	Test 3	Test 4	Test 5
γ_l	1.4	3.0	1.4	1.4	3.0
γ_g	1.4	1.35	1.4	1.4	1.4
π_l	0.0	3400.0	0.0	0.0	10.0
π_g	0.0	0.0	0.0	0.0	0.0
x_0	0.5	0.5	0.5	0.5	0.5

(b) Liquid phase

Test	α_{L_l}	ρ_{L_l}	u_{L_l}	p_{L_l}	α_{R_l}	ρ_{R_l}	u_{R_l}	p_{R_l}
1	0.8	1.0	0.0	1.0	0.3	1.0	0.0	1.0
2	0.2	1900.0	0.0	10.0	0.9	1950.0	0.0	1000.0
3	0.8	1.0	0.75	1.0	0.3	0.125	0.0	0.1
4	0.8	1.0	-2.0	0.4	0.5	1.0	2.0	0.4
5	0.6	1.4	0.0	2.0	0.3	1.0	0.0	3.0

(c) Gas phase

α_{L_g}	ρ_{L_g}	u_{L_g}	p_{L_g}	α_{R_g}	ρ_{R_g}	u_{R_g}	p_{R_g}
0.2	0.2	0.0	0.3	0.7	1.0	0.0	1.0
0.8	2.0	0.0	3.0	0.1	1.0	0.0	1.0
0.2	1.0	0.75	1.0	0.7	0.125	0.0	0.1
0.2	1.0	-2.0	0.4	0.5	1.0	2.0	0.4
0.4	1.4	0.0	1.0	0.7	1.0	0.0	1.0

Table 1 One-dimensional shock tubes. EOS parameters, initial discontinuity position and initial data for liquid and gas phases.

large variations of initial data and non-ideal equation of state. In test 3 the solution, for both phases, consists of a right shock wave, a right traveling contact discontinuity and a left sonic rarefaction wave. The correct resolution of the sonic point is very important in assessing the entropy satisfaction property of the numerical scheme. In test 4 both solid and gas phases consist of a two symmetric rarefaction waves and a trivial stationary contact wave. The region between the rarefaction waves is close to vacuum, therefore this test case is useful to assess the pressure positivity in different numerical methods. Test 5 was designed to assess the ability of numerical methods to resolve the stationary isolated contact waves. The exact solution allows the existence of the stationary contact waves in the solid and gaseous phases when the volume fraction and solid pressure gradients are present across the solid contact. The solution of this test problem contains isolated contacts in both solid and gas phases.

A comparison is made between a first order discretization (which corresponds to a classical Finite Volume approach) and a sixth order discretization, both with 100 elements. A solution obtained with a first order full non linear Riemann solver [30] on a mesh consisting of 2000 elements is shown for comparison. Results are shown in Fig. 1 where the mixture density is displayed ($\rho_m = \alpha_l \rho_l + \alpha_g \rho_g$). Final time has been set to $t = 0.15$ for tests 1 to 5. When the spatial discretization uses a first order representation of the solution, the Rusanov flux, although robust, does not give satisfactory results in the sense that it dissipates too much discontinuities. On the contrary, when the polynomial degree $N = 5$ is used, the solution is almost indistinguishable from the reference solution. It is remarkable how the artificial viscosity approach, detailed in Sec. 2.3, achieves to impose a very controlled amount of viscosity, keeping very sharp fronts and almost no oscillations.

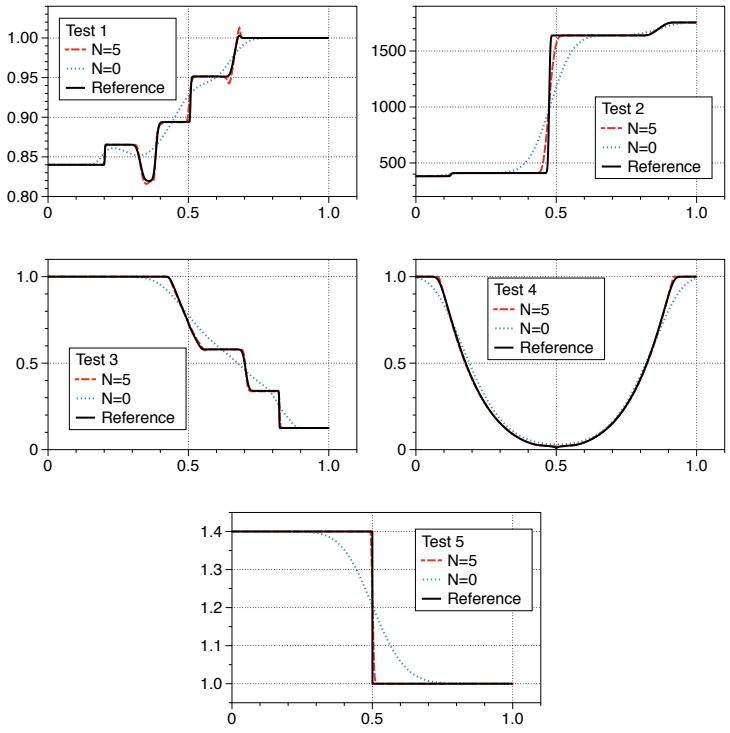

Fig. 1 Shock tube problems. Comparison between first order Rusanov with 100 elements, sixth order Rusanov with 100 elements and full non linear Riemann solver with 2000 elements. Density mixture.

4 Conclusions

In this work a discontinuous Galerkin discretization of the Baer-Nunziato equations that takes the DGSEM as a basis was introduced. The condition of Abgrall was used to extend the Rusanov flux to high order and to treat the non-conservative products. A stabilization technique based on local artificial viscosity was adapted to the Baer-Nunziato equations to deal with the inherent oscillations caused by high-order discretizations in the vicinity of discontinuities. This approach allowed to smooth the discontinuities in a very thin region and thus resolve them in the space of polynomials. The numerical experiments showed that the proposed discretization allows very high-order solutions in the presence of discontinuities. It was also shown that the accuracy of these solutions is comparable to the ones obtained with a full non linear Riemann solver with more than three times the number of degrees of freedom of the high-order counterpart.

Acknowledgements

This work has been partially supported by REPSOL under the research grant P130120150 monitored by Dr. Angel Rivero. This work has been partially supported by Ministerio de Economía y Competitividad (Spain) under the research grant TRA2015-67679-C2-2-R. The authors would like to thank the anonymous reviewers for their comments and suggestions which greatly improved this work.

References

1. Abgrall, R.: How to prevent pressure oscillations in multicomponent flow calculations: A quasi conservative approach. Journal of Computational Physics **125**, 150–160 (1996)
2. Arnold, D.N., Brezzi, F., Cockburn, B., Marini, L.D.: Unified analysis of discontinuous Galerkin methods for elliptic problems. SIAM Journal on Numerical Analysis **39**(5), 1749–1779 (2001)
3. Baer, M., Nunziato, J.: A two-phase mixture theory for the deflagration to detonation transition (DDT) in reactive granular materials. International Journal of Multiphase Flow **12** (1986)
4. Baldwin, B., MacCormack, R.: Interaction of strong shock wave with turbulent boundary layer. In: Proceedings of the Fourth International Conference on Numerical Methods in Fluid Dynamics, pp. 51–56. Springer (1975)
5. Black, K.: Spectral element approximation of convection–diffusion type problems. Applied Numerical Mathematics **33**(1-4), 373–379 (2000)
6. Canuto, C., Hussaini, M.Y., Quarteroni, A., Zang, T.A.: Spectral Methods. Fundamentals in Single Domains. Springer (2006)
7. Chaudhuri, A., Jacobs, G., Don, W., Abbassi, H., Mashayek, F.: Explicit discontinuous spectral element method with entropy generation based artificial viscosity for shocked viscous flows. Journal of Computational Physics **332**, 99–117 (2017)
8. Cockburn, B., Karniadakis, G.E., Shu, C.W.: The development of discontinuous Galerkin methods. Springer, Berlin, Heidelberg (2000)
9. Dormand, J.R., Prince, P.J.: A family of embedded Runge-Kutta formulae. Journal of computational and applied mathematics **6**(1), 19–26 (1980)
10. Douglas, J., Dupont, T.: Interior Penalty Procedures for Elliptic and Parabolic Galerkin Methods. In: Computing methods in applied sciences, pp. 207–216. Springer Berlin Heidelberg, Berlin, Heidelberg (1976)
11. Fraysse, F., Redondo, C., Rubio, G., Valero, E.: Upwind methods for the Baer–Nunziato equations and higher-order reconstruction using artificial viscosity. Journal of Computational Physics **326**, 805–827 (2016)
12. Gottlieb, D., Hesthaven, J.S.: Spectral methods for hyperbolic problems. Journal of Computational and Applied Mathematics **128**(1), 83–131 (2001)
13. Gottlieb, D., Orszag, S.A.: Numerical analysis of spectral methods: theory and applications. SIAM (1977)
14. Gottlieb, D., Shu, C.W.: On the Gibbs phenomenon and its resolution. SIAM review **39**(4), 644–668 (1997)
15. Hesthaven, J.S., Warburton, T.: Nodal discontinuous Galerkin methods: algorithms, analysis, and applications. Springer Science and Business Media (2008)
16. Hughes, T.J., Franca, L., Mallet, M.: A new finite element formulation for computational fluid dynamics: I. Symmetric forms of the compressible Euler and Navier-Stokes equations and the second law of thermodynamics. Computer Methods in Applied Mechanics and Engineering **54**(2), 223–234 (1986)

17. Jameson, A., Schmidt, W., Turkel, E.: Numerical solution of the Euler equations by finite volume methods using Runge Kutta time stepping schemes. In: 14th fluid and plasma dynamics conference, p. 1259 (1981)
18. Kirby, R.M., Sherwin, S.J.: Stabilisation of spectral/hp element methods through spectral vanishing viscosity: Application to fluid mechanics modelling. Computer methods in applied mechanics and engineering **195**(23), 3128–3144 (2006)
19. Klöckner, A., Warburton, T., Hesthaven, J.S.: Viscous shock capturing in a time-explicit discontinuous Galerkin method. Mathematical Modelling of Natural Phenomena **6**(3), 57–83 (2011)
20. Kompenhans, M., Rubio, G., Ferrer, E., Valero, E.: Adaptation strategies for high order discontinuous Galerkin methods based on Tau-estimation. Journal of Computational Physics **306**, 216–236 (2016)
21. Kompenhans, M., Rubio, G., Ferrer, E., Valero, E.: Comparisons of p-adaptation strategies based on truncation-and discretisation-errors for high order discontinuous Galerkin methods. Computers & Fluids **139**, 36–46 (2016)
22. Kopriva, D.A.: Implementing Spectral Methods for Partial Differential Equations: Algorithms for Scientists and Engineers. Springer (2009)
23. Lax, P.D.: Weak solutions of nonlinear hyperbolic equations and their numerical computation. Communications on Pure and Applied Mathematics **7(1)**, 159–193 (1954)
24. Parès, C.: Numerical methods for nonconservative hyperbolic systems: a theoretical framework. SIAM Journal on Numerical Analysis **44**, 300–321 (2006)
25. Persson, P.O., Peraire, J.: Sub-cell shock capturing for discontinuous Galerkin methods. Proc. of the 44th AIAA Aerospace Sciences Meeting and Exhibit **AIAA-2006-112** (2006)
26. Rasetarinera, P., Hussaini, M.Y.: An Efficient Implicit Discontinuous Spectral Galerkin Method. Journal of Computational Physics **172**(2), 718–738 (2001)
27. Reed, W.H., Hill, T.R.: Triangular mesh methods for the neutron transport equation. Los Alamos Report LA-UR-73-479 (1973)
28. Rusanov, V.V.: The calculation of the interaction of non-stationary shock waves and obstacles. USSR Computational Mathematics and Mathematical Physics **1(2)**, 304–320 (1961)
29. Saurel, R., Abgrall, R.: A multiphase Godunov method for compressible multifluid and multiphase flows. Journal of Computational Physics **150**(2), 425–467 (1999)
30. Schwendeman, D., Wahle, C., Kapila, A.: The Riemann problem and a high-resolution Godunov method for a model of compressible two-phase flow. Journal of Computational Physics **212**(2), 490–526 (2006)
31. Tadmor, E.: Convergence of spectral methods for nonlinear conservation laws. SIAM Journal on Numerical Analysis **26**(1), 30–44 (1989)
32. Tokareva, S., Toro, E.: HLLC-type Riemann solver for the Baer–Nunziato equations of compressible two-phase flow. Journal of Computational Physics **229**(10), 3573 – 3604 (2010)
33. Toro, E.F.: Riemann Solvers and Numerical Methods for Fluid Dynamics. A Practical Introduction. Springer (2009)
34. Von Neumann, J., Richtmyer, R.D.: A method for the numerical calculation of hydrodynamic shocks. Journal of applied physics **21**(3), 232–237 (1950)
35. Wang, Z.: High-order methods for the Euler and Navier–Stokes equations on unstructured grids. Progress in Aerospace Sciences **43**(1), 1–41 (2007)
36. Winters, A.R., Kopriva, D.A.: High-order local time stepping on moving DG spectral element meshes. Journal of Scientific Computing **58**(1), 176–202 (2014)